

THERMAL DECOMPOSITION OF EVA COMPOSITE ENCAPSULANT OF SINGLE JUNCTION AMORPHOUS SILICON PHOTOVOLTAIC (PV) MODULE

G. O. OSAYEMWENRE*, E. L. MEYER

Fort Hare Institute of Technology (FHIT), University of Fort Hare

The EVA, decomposition of single junction amorphous silicon solar module (a-Si:H) observed during outdoor deployment has been studied. The decay and thermal breakdown of EVA in the encapsulating material of PV module is a sign of low quality in thin film solar cell. The decomposition of EVA due to localized heating affects the reliability and efficiency of PV module. It also has negative influence on the conductive ZnO₂ layer and the heat dissipating mechanisms of the PV module. The thermal susceptibility and stability of the encapsulating material was investigated using Thermogravimetric (TGA), result shows low quantity of EVA substance in the affected region due to loss of volatile substance from the affected region after decomposition.

(Received September 17, 2014; Accepted November 21, 2014)

Keyword: Thermogravimetric (TGA); SEM; Photon; Ethylene-vinyl acetate

1. Introduction

The quantity of light utilized by solar cell is a fraction of the total incident sunlight which reaches the surface of the cell. Sunlight consists of discrete packets of light ray; these packets are made up of photon and only photon of the right frequencies are converted to photo-generated current. Most of the photons absorbed by the solar cell surface results into thermal energy [1]. Therefore there must be a proper heat dissipating channel, to prevent an abnormal rise in the junction temperature [1-2]. This is why the efficiency of solar cells is usually low; some are normally between 14-19%, except for multi-junction-Si cell, which is about 34% [3-4]. It is necessary for the encapsulating material of PV module to be thermally stable so as to be able to resist the presence of focal heat.

In general solar cell encapsulating material consists of Glass/Ethylene-vinyl acetate (EVA) /ARC-Si/EVA/Tedlar [5-6].

The photovoltaic (PV) module used in this study is the single junction amorphous silicon (a-Si) module. Figure 1 shows a close view of one of the modules, the scribe lines appear as gray horizontal lines. These lines are approximately 1.0 millimeter wide and separate adjacent cells from each other's. The cells have been monolithically connected in series during the manufacturing stage. The module comprises of 29 series connected cells and has an aperture area of (0.920 x 0.125) m².

* Corresponding author: gosayemwenre@ufh.ac.za

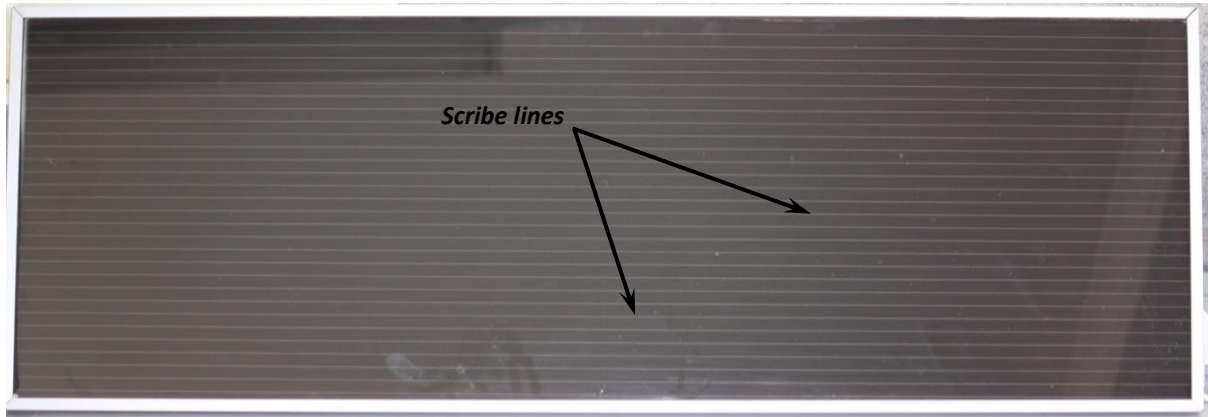


Fig. 1. Illustration of the 29 monolithically connected cells in the a-Si: H module 1

Generally, amorphous silicon modules are prone to degradation mode, though there are various causes of degradation, but this study limits its scope to the degradation caused by the poor encapsulating material. In this venture, focus is on the thermal decomposition of EVA. The term thermal decomposition refers to the decay/breakdown of EVA encapsulating material. This study also presents the chemistry of EVA and calculation showing the loss of EVA in the encapsulating material.

2. Theory

2.1. Effect of EVA decay on series resistance

One source of power loss in PV module is the presence of structural deformation, which occurs in the affected region. Sometime this morphological defect is caused by a hot spot formation. As structural damage continues, some part of the cell experience thermal decomposition leading to a total breakdown of the EVA [9]. The thermal energy required for this process is derived from the localized heating of the region, due to hot spot formation [7]. During this process, a simultaneous thermal oxidation process starts around the module edges. This process leads to an increase in the module series resistance [7-9], hence a reduction in the generating power because the affected cell, acts as a reverse biasing cell to the string current. An increase in series resistance causes the cell to dissipate more power in overcoming the resistance before current can flow.

Theoretically series resistance does not affect I_{sc} but effects the fill factor (FF) and the solar cell efficiency (η), according to the following equation 1 & 1.1 [10].

$$FF = \frac{I_{Max} V_{Max}}{I_{SC} V_{OC}} \quad (1)$$

$$\eta = \frac{P_{max}}{P_{sun}} = FF \frac{I_{SC} V_{OC}}{P_{Ssun}} \quad (1.1)$$

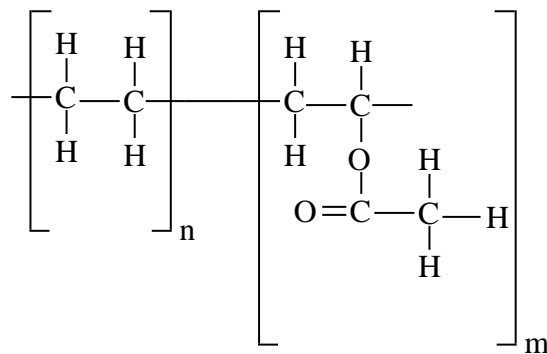
I_{sc} is the short circuit current, V_{oc} is the open voltage, I_{max} is the maximum current, V_{max} is the maximum voltage, P_{max} is the maximum power, P_{sun} is the solar power depending on the irradiance, FF is the fill factor and η is the solar efficiency.

The morphological damage observed in Fig. 3, affect the internal layer of the cell, this in turn can affect the p-i-n layer, the metal contact and metal contact resistivity. Hence, the resistance

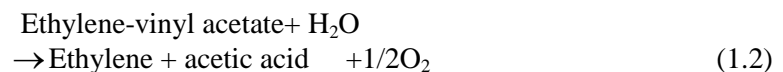
of the junction and the silicon to metal contact increases. The above theory is justified by the fact that series resistance is affected by; the flow of current through the p-i-n junction and the resulting resistance across the metal to silicon contact [3, 10-11].

2.1. Chemistry of EVA (decomposition)

Ethylene-vinyl acetate has a molecular formula of $\text{CH}_3\text{COOCH}=\text{CH}_2$ [5, 7-8], why its structural formula is represented below.



When ethylene-vinyl acetate decomposed, it yields Ethylene and acetic acid (which is a volatile acid). This process can be either through oxidation in the presence of vapour or through thermal medium, as represented by equation 1.2 and 1.3.



Ethylene is a hydrocarbon with a molecular formula C_2H_4 ($\text{H}_2\text{C}=\text{CH}_2$). The molar weight of acetate (CH_3COOH) is 60.05g/Mol, when acetate reacts with the surrounding atoms depending on the mode of decomposition it can produce overtones [12-14].

3. Experimental and methods

Fig. 2 shows the five modules (red outline) on the north-facing test rig, at an angle of 34° , the latitude of the site. These modules were first mounted outdoors on 27 September 2012. The other modules on the test rig as well as the grid-independent building in the background, formed part of other studies outside the scope of the present one. The electrical characterization of the modules was done using IV tracer, to establish the degradation process [25].



Fig. 2: Outdoor monitoring of different PV modules on the rack, the red link indicate the investigating modules

3.1. Structural Diagnostics

The module (1) was diagnosed for structural defect. For this analysis, two samples were prepared, one from the affected region and the other from the non-affected region. The classification of the region into affected and non-affected is derived from the following analysis, [i] vision inspection and [ii] infrared (IR) thermo-graphical analysis [23, 25]. Some areas of the affected regions are transparent due to the decomposition (decay) of EVA in those spots. The optical microscopic image and the visual inspection in figure 3 show these decompositions.

The morphological analyses of the module were determined using JEOL JSM- 6390LV optical scanning electron microscopy and the field emission phonon scanning electron microscopy (higher resolution). The samples were cut into smaller size of (15×15) mm and placed on the stubs using carbon double side tab. The samples were cleaned with a compressed air and dried at an ambient condition (25 °C). The prepared sample was later introduced into the SEM device under an acceleration voltage of 15 KV.

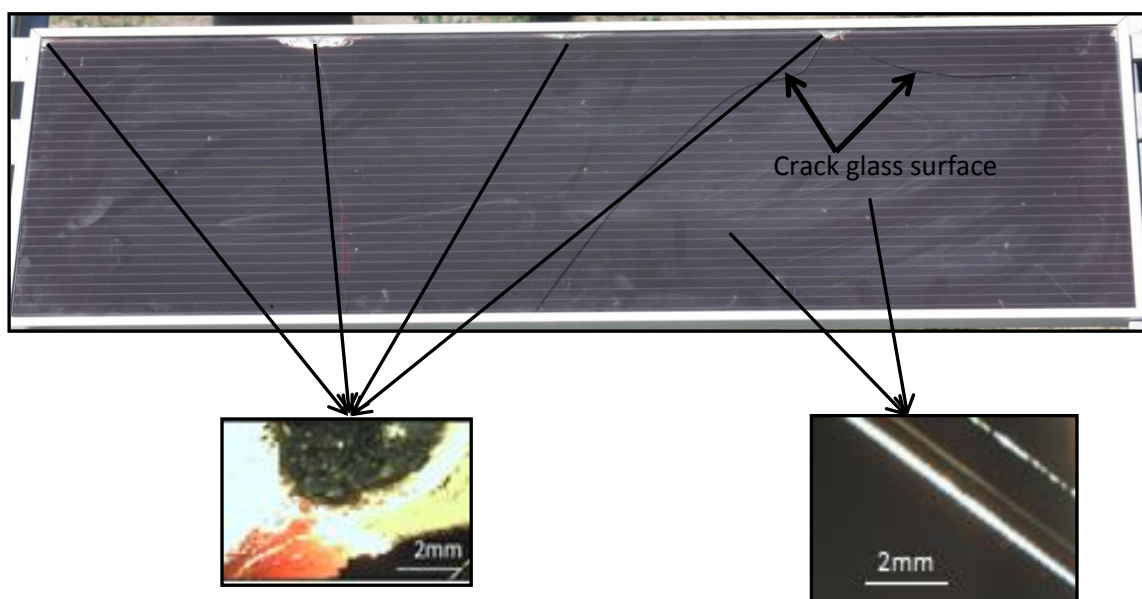


Fig. 3. Represent the actual visual change observed, also shown are affected region and non-affected region with the aid of electron microscope (EM)

3.2. Chemical Kinetics

3.2.1. Thermo-gravimetric Analysis (TGA)

This method gives qualitative information about the thermal stability of the material (EVA). At the end of week 28 the degree of damage in module 1 increased, why some region shows sign of EVA decay. This decomposition of the encapsulating material in module 1 necessitated the use of thermo-gravimetric analysis. For this study an Afrox thermo-gravimetric analyzer 7 was used with nitrogen (20°C) as the baseline gas at 1 atmospheric pressure. The operating condition of the analyzer includes temperature range, from 20°C to 900°C at 10°C/min while the gas flowing rate was 10 ml/min. Two samples were prepared for analysis, one from the affected region and the other from non-affected region. These samples are subsample of the samples used for the SEM analysis. The weight of the each sample was 21.337 mg, to have an optimal result the weight of the samples should be between 21-22 mg. Finally the thermal stability of the encapsulating layer (EVA), were evaluated from equation 2.1[15]:

$$VA = \text{Wt loss of acetic acid} \times \frac{\text{Mwt of VA}}{\text{Mm of acetic acid}} \quad (2.1)$$

where VA is the Vinyle acetate, while Mwt is the molecular weight and Mm is the molecular mass.

4. Result and discussions

4.1 SEM Results showing EVA decay

The SEM micrographs of the samples are shown in figure 3. These diagrams illustrate the effect of localized heat on the surface morphology of the module. Figure 3b is the magnified version of 3a and it demonstrates the absence of EVA in the circled portion of the affected region. The figure 3 also shows the presence of severe burn area in this region due to thermal decomposition of the EVA. The surface morphological structure as well as the packing density decreased in the affected region when compared to the non-affected, this mean the optical density degradation will varies according to the degree of damage in the region. Figure 3c is a micrograph image from phonon SEM of a higher resolution

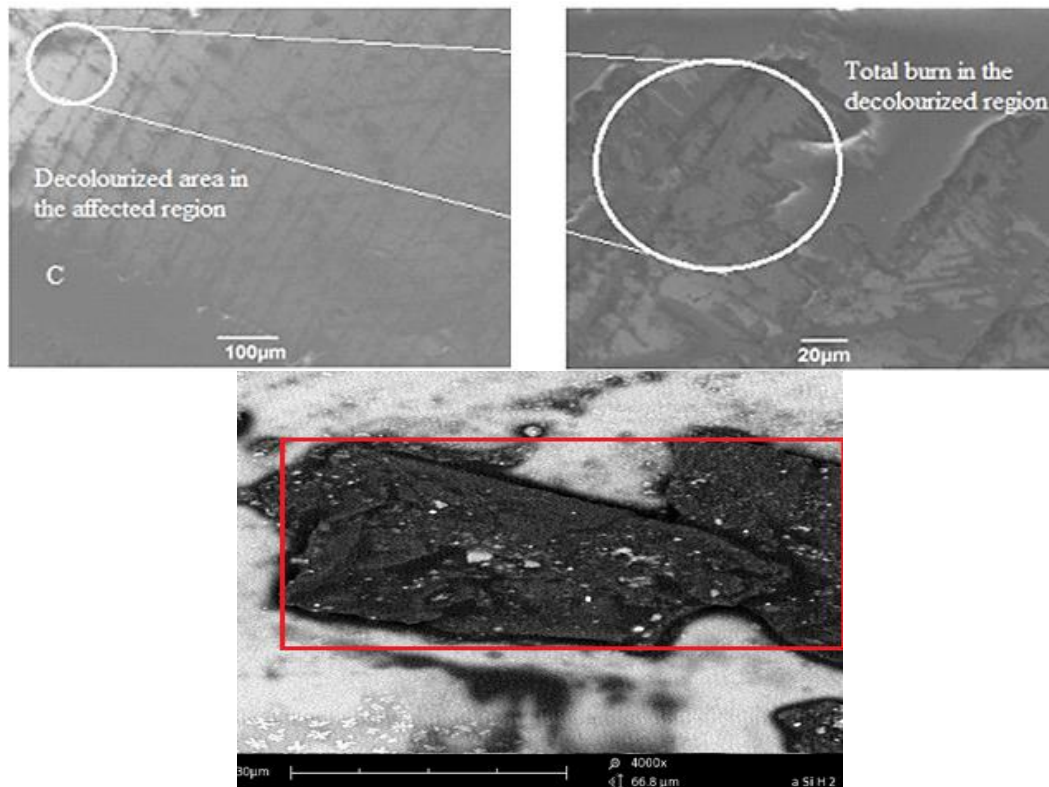


Fig. 3. SEM micrographs of (a) samples from the affected region with surface glass and (b) showing the depletion of encapsulating material after delamination of the sample (c) higher resolution of sample from after region before delamination

Fig. 3 show the structural damages of the affected region in the module. The area marked in each micrograph, illustrates the region of decomposition of the encapsulating layers.

4.2. Thermogravimetric Analysis

Fig. 4 presents the thermal stability result. Figure 4 compares the EVA content of the affected region to that of the non-affected region. It is clear that decomposition of EVA is responsible for weight loss in the affected region. For the non-affected region a temperature range of 180°C-792°C was used and the calculated VA (%) was 2.511g. However for a temperature range of 32°C -792°C, (were the initial weight (%) is 100 and the final weight (%) is 98.104) the VA (%) loss becomes 2.717g but between 32°C and 180°C, the observed weight % loss is attributed to the presence of volatile substance. In the affected region a temperature range of 180 °C to 792 °C was also used and the calculated VA (%) was 0.701g. Between 32 °C to 180 °C, no weight loss was observed. The entire volatile component has been loss through evaporation as a result of the total destruction of the module back cover.

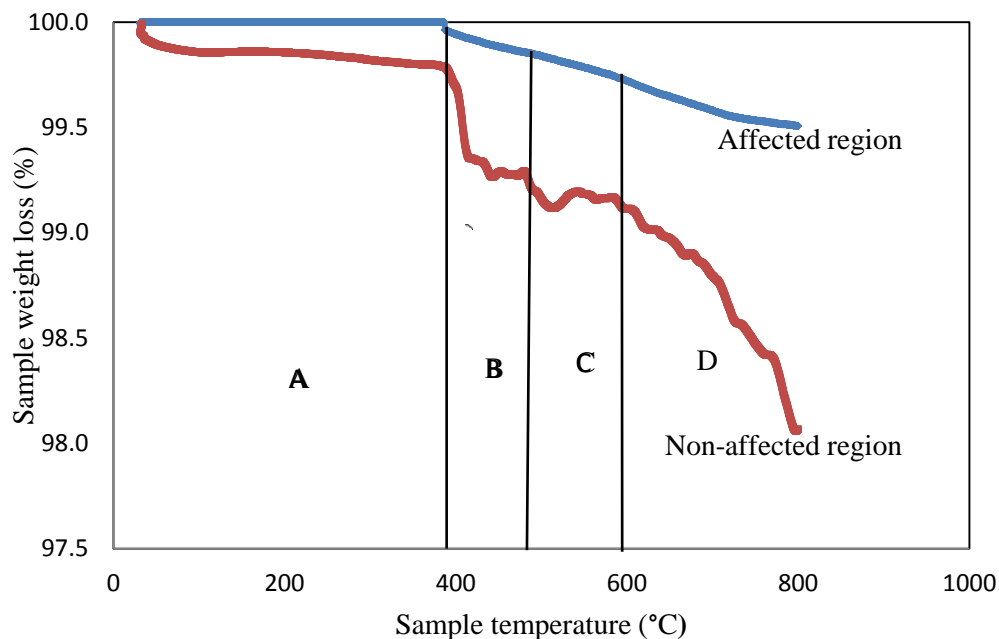
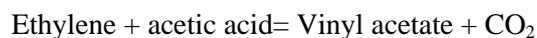


Fig. 4. TGA analysis of the affected and non-affected regions of single junction amorphous module

EVA acts as a convectional barrier for collectors (absorbent material) in solar cells. Han and Kummar [2003], proved that the thermal decomposition (combustion) of ethylene is the main source of carbon iv oxide loss, as shown in the chemical reaction below.



There are two possible processes for ethylene combustion. First, from the dissociation of C_2H_4 to give Carbon plus Hydrogen, in the presence of oxygen combustion start, resulting in CO (incomplete combustion), CO_2 , and H_2O formation [18]. The second method is the remover of H from C_2H_4 by highly energetic activated oxygen to form CO, CO_2 and H_2O (O-H, C-O) bond [16-18].

The deviation in the graph (standard GTA graph) is due to the microstructural disorder nature of the sample which is a characteristic of an amorphous material [19-20]. Regions A, B, C, D represent the transition phase; A is the solid state, B is melting phase, C is the liquid stage while D is the vapour state [20]. The decrease in weight % as seen in the affected regions is due to the formation of CO_2 , and H_2O which are later given off as temperature increases.

4.2.1. Thermal decomposition of Polymer (EVA/Vinyl Acetate)

As shown from Fig. 4 the weight loss from the non-affected region is more than the affected region. This is attributed to the vaporization of volatile component of EVA after decomposition. In this study the heat generated from localized heating (hot spot) provides the thermal energy for this process. The presence of thermal energy leads to two important phenomena which are; thermal decomposition and thermal degradation. According to American Society for Testing and Materials (ASTM) [21], 'thermal degradation is a chemical change which occurs in a material as a result of increase in temperature. At the end of the process the material losses its mechanical, physical and electrical properties' [22]. While thermal decomposition is a chemical reaction, which involves the breaking down of material into its smaller unit as a result of heat. The thermal degradation explained above is an endothermic reaction, as long as there are hot spots in this region the process will continue until the region is completely destroyed. Since the localized heat is acting as a form of feedback and provides sufficient heat to this region, the process will continue.

In general, the thermal decomposition of polymer starts from oxidation process, the presence of an oxidizing agent increases the thermal decomposition. When heat precedes thermal decomposition, in the presence of oxidant like oxygen or air, the rate of decay or decomposition will increase [22]. The presence of oxidant reduces the decomposition temperature of the polymer, hence we expect rapid decomposition. This explains why the observed EVA decomposition continues even during the period when the ambient temperatures were low. Since hot spot regions are characterized by high oxygen content [23], this oxygen impurity together with the surrounding oxygen will act as an oxidant to the decomposition process.

The life span of EVA is about 20-35 years; hence a lifetime of 16 months is an indication of low quality material. The high oxygen content inside the device has the capability to diffuse into the encapsulant, [14, 18]. Brauman, [14] and Gijsman [18], demonstrated that oxygen is able to travel down inside a device (EVA) up to a distance of 10mm. While Cullis [14], Hirschler [24], Simon et al; [16] and Gijsman et al [1988], established that the rate of thermal decomposition is influenced by the presence of oxygen.

5. Conclusions

Our findings show the decomposition of the encapsulating layer of a-Si:H, due to localized heating. The quantity of EVA therefore decreases in the affected region because of thermal decomposition. The production of CO₂ and H₂O are responsible for the less quantity of VA in the affected regions. The thermal decomposition is responsible for the damage observed in figure 3 once this happens, the intrinsic layer becomes naked to harmful UV radiation hence the module will continue to experience degradation.

Acknowledgement

The authors wish to acknowledge DST, ESKOM, GMRDC at the University of Fort Hare for financial support, and Dr Sampson M for his encouragement during this work.

References

- [1] Y. Tripanagnostopoulos, T. Nousia, M. Souliotis, et al., *Solar Energy* **72**, 217 (2002).
- [2] A. Royne, C. J. Dey, D. R. Mills, A critical review. *Solar Energy Materials and Solar Cells* **86**, 451 (2001).
- [3] M. Mathias, at (<http://energyinformative.org>) accessed 23/02/2014.
- [4] M. A. Green, K. Emery, Y. Hishikawa, W. Warta, E. D. Dunlop, *Progress in Photovoltaics: Research and Applications*, **22**, 1-9 (2014).
- [5] R. B. Seymour, C. E. Carraher, Jr., *Polymer Chemistry*, Marcel Dekker, Inc., New York. 519(1988).
- [6] C. Andre's, F. Maxime, F. Rougieux, and D. Macdonald, *International Conference on materials for Advance Technology, symposium*, (2011).
- [7] Y. F. Han, D. Kummar, C. Sivadinarayana, D. W. Goodman, *Journal of Catalysis* **224**, 60, 2008 (2003).
- [8] S. K. Brauman, *J. Polymer Science B* **26**, 1159 (1988).
- [9] T. Kashiwagi, H. Nambu, *Combust Flame* **88**, 345 (1992).
- [10] E. L. Meyer and E. E. van Dyk, *IEEE Trans. Reliability* **53**, 83 (2004).
- [11] A. Q. Malik et al, *Journal of Applied Physics* **72**, 253 (1998).
- [12] C F. Cullis, M. M. Hirschler, Oxford University Press, Oxford, UK (1981).
- [13] G. Roscher, *Vinyle Esters IN ullmann's Encyclopedia of Cemical Technology*, John Wiley & Sons: New York (1981).
- [14] S. K. Brauman, *J. Polymer Science B* **26**, 1159 (1981).

- [15] J. Chiu, Appl. Poly. Sym. **2**, (1996).
- [16] P. Simon et al., Polymer Degradation Stability **29**, 253 (1992).
- [17] P. J. Gijsman, J. Vincent et al, Polymer Degradation and Stability **42**, 95 (1993).
- [18] R. Wang, D. Merz,. Phy. Stat. Sol. A **39**, 697 (1977).
- [19] D. Turnbull, J. Phys. C **35**, 401 (1974).
- [20] M. I. Ojovan. Journal of Experimental and Theoretical Physics Letter **79**, 632 (2004).
- [21] ASTM E 176, American Society for Testing and Materials, West Conshohocken, PA, 4.07.
- [22] L. B. Craig and M. M. Hirschler, SFPE Handbook of Fire Protection Engineering **C 7**, (2008).
- [23] M. Simon, PhD Thesis, Fort Hare University, 132-142 (2009).
- [24] M. M. Hirschler, Europ. Polymer J. **18**, 463 (1982).
- [25] G. O. Osayemwenre MSc thesis, Fort Hare University (2014).